Discover Oceans

RESEARCH Open Access

Community dynamics and functional traits drive microplastic sequestration by marine nematodes

Flávia Juliana Lobato de França[1*], Renan Belém da Silva[1], Débora Alissandra de Araujo França[1], Iully Durão Frasson[1], Gustavo André Xavier da Silva[1], Maria Eduarda Lima Rodrigues[1], Giovanna Lins Pessoa[1], Anna-Maria Vafeiadou[2], Tom Moens[2] and Giovanni Amadeu Paiva dos Santos[1*]

*Correspondence:
flaviah.lobato@hotmail.com;
giopaiva@hotmail.com

[1] Center for Biosciences, Department of Zoology, Universidade Federal de Pernambuco, Campus Recife, Recife, Pernambuco, Brazil
[2] Marine Biology Lab, Biology Department, Ghent University, Ghent, Flanders, Belgium

Abstract

Benthic sediments are recognized as the principal sink for the 'missing plastic', yet the biological processes governing microplastic (MP) fate within this reservoir remain critically unresolved. Here, we investigate whether and how marine nematode communities, the most abundant metazoans in marine sediments, influence the fate and ecological risk of MPs. Using short-term (9-day) and long-term (30-day) microcosm experiments, we assessed the influence of MP density and exposure time on nematode community structure, functional diversity, and sequestration capacity. Our results reveal that MP sequestration by nematodes only manifests at very high-MP densities. Counter-intuitively, the most severe impacts on nematode communities occurred at low MP densities, despite particle uptake remaining below detection there. The magnitude of the sequestration role of the nematode community heavily depended on nematode functional characteristics, with opportunistic non-selective ingesters being responsible for 90% of the MP sequestration in the short-term experiment. With a structurally very different community at the start, MP uptake in the long-term experiment was considerably lower and shared by a functionally more diverse consortium of more K-selected taxa with diverse feeding strategies, but all having fairly wide buccal cavities. Our study reveals that nematode communities are an active and dynamic biological compartment where MPs are processed, transformed, and reintroduced into the food web, but the quantitative importance of their role in trophic transfer appears very limited.

Keywords: Meiofauna, Benthic food web, Ecological risk, Plastic cycle, Functional diversity

1 Introduction

Plastic pollution is a pervasive environmental challenge, with debris documented across all marine ecosystems [1–4]. Global production has generated over six billion tons of plastic waste deposited into the environment [5]. Cumulative inputs to the oceans were projected to reach 155 million tons by 2025, a figure that compounds this legacy [6]. In the marine realm, this material fragments into ubiquitous microplastics (MPs), particles smaller than

5 mm [7, 8]. This fragmentation dramatically increases their bioavailability and the complexity of tracking their environmental pathways [1].

A critical inconsistency persists in our understanding of the global plastic cycle. The mass of MPs in surface waters is orders of magnitude lower than predicted by ocean-input models, a discrepancy termed the 'missing plastic' paradox [9, 10]. This suggests that the ocean surface serves as a transient reservoir and that a significant fraction of plastic pollution is transported to the seafloor [11]. Marine sediments are now recognized as the principal global sink, potentially sequestering 70 to 90% of all plastic entering the ocean [2, 12]. This vertical transport is driven by mechanisms including the direct sinking of high density polymers such as polyethylene terephthalate (PET) and polyvinyl chloride (PVC) and, crucially, the biofouling of buoyant polymers like polyethylene (PE) and polypropylene (PP), which increases their density and facilitates sedimentation [13–16].

However, the seafloor is not an endpoint but the start of a new biogeochemical cycle, where the ultimate fate of MPs, whether burial, resuspension, or trophic transfer, is governed by the activity of benthic organisms. Among the benthic fauna, meiofauna, a diverse assemblage of microscopic metazoans, are uniquely positioned to interact with, and influence the fate of, MPs due to their size and intimate association with sediment particles [17]. Within this group, free-living nematodes are the most abundant and diverse metazoans in marine sediments globally, often comprising over 90% of individuals and acting as a critical link in benthic ecosystems [18, 19]. The ecological significance of nematodes is multifaceted. As microscale ecosystem engineers, they actively restructure sediment through bioturbation, making them primary modulators of the vertical distribution of contaminants [20]. Concurrently, nematodes occupy a central position in the benthic food web, channeling energy from microbial and detrital pools to higher trophic levels [19, 21]. This dual role establishes them as a potential bottleneck or conduit for MP transfer within benthic ecosystems.

Direct ingestion of MPs by nematodes is a confirmed pathway [22–24]. However, the collective consequence of these interactions at the community level, and their impact on the ecosystem-scale fate of MPs, remain a critical and unexplored knowledge gap. The functional diversity of nematodes, reflected in their varied buccal morphologies and life-history strategies, suggests that their effects on and responses to MPs are not uniform. This functional heterogeneity could lead to complex outcomes, from physiological harm to individuals [25] and community restructuring [26] to profound alterations in ecosystem-level energy flow and contaminant transfer [27]. To address this knowledge gap, our study investigates the integrated role of the nematode community as a biological sink, assessing its structural and functional responses to determine the ecosystem-level consequences of MP exposure.

Using a combination of short-term and long-term exposure experiments, we specifically sought to understand this role and how it evolves from the initial toxicological response and specialist-driven function to the potential for community adaptation and functional succession. Specifically, we aimed to: (1) quantify the MP sequestration capacity of the nematode community and determine how its structure is altered by MP exposure; (2) use a functional-trait approach to identify the nematode taxa that are the primary drivers of MP sequestration; and (3) provide an order-of-magnitude estimate of the quantitative significance of gut storage for the transfer of MPs to higher trophic levels. We formulated

hypotheses grounded in the established principles that environmental contaminants act as selective pressures on communities [28], and that the functional traits of nematodes are good predictors of their ecological roles [29]. Based on this framework, we tested the following: (H1) MP exposure will reduce nematode density and diversity, selecting for tolerant, opportunistic taxa and thereby altering the community's collective capacity to act as a biological sink and (H2) nematodes with r-like life strategies and non-selective feeding behaviors supported by wide buccal cavities will ingest MP at higher rates and be gateways for MP entry into the benthic food web. Addressing these questions is essential for developing a mechanistic and quantitative understanding of the role of benthic fauna in the global plastic cycle.

2 Materials and methods

2.1 Study area and sampling

The nematode community was sourced from intertidal sediments at Cupe Beach, located in Ipojuca, Pernambuco, Brazil (8°27′29.4"S 34°59′03.2"W), during the summer low tides of the 2022–2023 period. The depositional site was selected for its fine-grained sand matrix and well-characterized meiofauna community [22], which provided an ideal natural system for microcosm studies. Samples were collected by scraping the top 2 cm of sediment, the zone of highest meiofaunal abundance and biological activity [30]. To create a uniform sample, the collected sediment was gently homogenized and transported to the laboratory in aerated containers with site-sourced seawater. To minimize stress from collection and ensure a stable baseline community, the sediment was maintained under controlled laboratory conditions (28 °C, 35 salinity) for a seven-day acclimatization period before initiating the experiments [31, 32]. During this period, sediment was kept in a single large, aerated aquarium. No external food was added, as the natural sediment contained sufficient organic matter to sustain the community [22, 32].

2.2 Microcosm setup

To investigate both short-term and long-term responses, two independent experiments were conducted over 9 and 30 days, respectively. The experimental design was based on the microcosm set-up established by Vafeiadou et al. (2018) and validated in our previous research [22]. In brief, each microcosm was prepared in a glass beaker containing a 5–6 cm layer of sediment submerged in 0.2-µm-filtered seawater. This sediment comprised a homogenized mixture of 300 g of natural, live sediment and 100 g of defaunated sediment. The sediment was defaunated by freezing (−20 °C for 48 h) and subsequent thawing, a method that eliminates metazoans while preserving at least part of the native microbial community [33, 34]. Each microcosm consisted of 400 g of sediment, prepared in a two-step process to ensure a homogeneous distribution of contaminants. First, the nominal density of MPs for each treatment was thoroughly mixed into 100 g of defaunated sediment. This portion served as a contaminated carrier matrix. Second,

this contaminated carrier was carefully and slowly homogenized with 300 g of natural, live sediment. This two-step method ensures a controlled and even introduction of MPs throughout the final sediment matrix while minimizing mechanical stress on the living organisms. A negative-pressure aeration system maintained oxygen at the sediment–water interface, preventing confounding effects of hypoxia/anoxia (for details on the design, see Vafeiadou et al., 2018). All microcosms were kept in a temperature-controlled room at 28 ± 1 °C and 35 ± 1 salinity. A total of 16 independent microcosms were prepared for each experiment (short- and long-term), representing four replicate beakers for each of the four treatment groups (Control, 10^3, 10^5, and 10^7 particles/mL). To prevent cross-contamination, the replicates of each treatment were placed in separate water baths (four water baths in total), all maintained under identical temperature and light conditions. The initial nematode density was not artificially standardized; instead, we ensured a homogeneous starting community by adding a standardized mass (300 g) of homogenized natural sediment to each replicate.

2.3 MP treatment and laboratory sampling

The contaminant source consisted of 1-µm diameter fluorescent polystyrene microspheres (Fluoresbrite®; excitation: 441 nm, emission: 485 nm) from Polysciences Europe GmbH (Germany). This specific size and shape were chosen for their ecological relevance to nematode feeding ecology. Polystyrene is a common polymer in marine pollution. The 1-µm spherical particles are within the optimal size range for ingestion by many bacterivorous and deposit-feeding nematodes [23, 35], mimicking the size of their natural bacterial prey. Furthermore, fluorescent spheres are a standard tool that allows for unambiguous quantification of ingestion. Nominal exposure densities of 10^3, 10^5, and 10^7 particles/mL of sediment were established. This range was designed as a tiered approach: the lowest density reflects levels found in moderately polluted coastal sediments [15, 16], while the higher densities represent expected future scenarios, enabling the construction of dose–response relationships and the identification of ecological thresholds. Detailed procedures for preparing the contaminated sediment via serial dilutions are described in de França et al. (2024). In summary, first, a stock slurry of MPs was mixed into a portion of defaunated sediment to create a highly concentrated carrier sediment (4×10^7 particles per 100 g). This mixture was manually homogenized for several minutes until visually uniform and allowed to settle for approximately 30 min. Second, this carrier sediment was either used directly or serially diluted with uncontaminated defaunated sediment to create the stock for each target concentration. Finally, 100 g of the appropriate contaminated sediment stock (or uncontaminated defaunated sediment for the control group) was homogenized with 300 g of live sediment to establish each microcosm. The homogeneity of the final mixture relies on this standardized, multi-step process; hence the concentrations are referred to as nominal. Sampling was conducted at multiple time points within the same replicate microcosms using a repeated-measures design. In the short-term experiment, sediment subsamples were carefully collected from each beaker at 3, 6, and 9 days (T3, T6, T9). These intervals were chosen to capture the rapid response of opportunistic nematodes with often short

(days to weeks) life cycles. Subsampling was performed using a transparent Perspex corer (3.6 cm inner diameter), which collects a surface area of approximately 10 cm^2. A similar procedure was followed for the long-term experiment, with subsampling at 15 and 30 days (T15, T30). This longer timescale was designed to assess chronic effects and potential ecological succession within the community, spanning multiple generations of both opportunistic and more persistent taxa. This design allowed us to track the temporal dynamics within each replicate, and we acknowledge that the subsampling itself introduces a minor, controlled disturbance.

2.4 Sample processing

Nematodes were extracted from sediment samples using a 300-µm sieve to remove macrofauna and a 38-µm sieve to retain meiofauna. The retained fraction was then subjected to centrifugation-flotation with Ludox HS40, a non-toxic silica polymer, to separate organisms from sediment particles [36]. The extracted nematofauna was first frozen while alive (−20 °C, 12 h); this step serves to relax the specimens for accurate morphometric measurements and to prevent the egestion of gut contents [37]. They were then preserved in 4% formaldehyde and stained with Rose Bengal to facilitate their detection and counting. Total nematode counts were performed under a stereomicroscope (Zeiss Stemi 305) using magnifications ranging from 16× to 64×. From each replicate, ca 130 nematodes were randomly picked and mounted on permanent slides using the glycerin-ethanol method [38]. Taxonomic identification to the genus level was performed under a compound microscope (Zeiss Scope A1) and 40× to 100× magnification, using established keys [39–41] and the Nemys database (Nemys eds. 2025). Identified genera were then assigned to functional groups. Trophic groups were assessed from buccal morphology [42] as: 1A (selective deposit-feeders), 1B (non-selective deposit-feeders), 2A (epistrate-feeders), and 2B (predators/omnivores). The Trophic Diversity Index (TDI) was calculated according to Heip et al. (1985) using the formula: $TDI = 1—\Sigma\theta^2$, where θ is the contribution of the density of each trophic group to the total nematode density. This index ranges from 0.25 to 1, where a higher TDI value indicates greater trophic diversity within the nematode community. Life-history strategy was assigned using the colonizer-persister (c-p) scale, which ranks genera from 1 (opportunistic colonizers with an r-selected life-history strategy) to 5 ('persisters' characterized by K-selected life-history traits) [43]. The community Maturity Index (MI), a weighted average of these c-p values, was calculated using the formula: $MI = \Sigma v(i) \times f(i)$, where v(i) is the c-p value of genus i, and f(i) is the frequency of that genus. This index is a robust indicator of ecosystem disturbance [44].

Biomass was determined for ca 100 individuals per replicate by measuring body length (L) and width (W) from images captured using ZEN software connected to a Zeiss Scope A1 microscope, and applying a slightly modified version of the Andrassy [45] formula: Biomass (µg wet weight) $= (L \times W^2 / 1.7) \times 1.13 \times 10^{-6}$. Ingested MPs were quantified in these same individuals using an epifluorescence microscope (Zeiss Scope.A1) at 40× magnification. The number of fluorescent microspheres was counted in three distinct body regions: anterior (pharynx), anterior intestine (gonadal region), and posterior

intestine (post-gonad to anus), providing a detailed account of particle distribution within the organism.

2.5 Data analysis

Multivariate analyses were performed on nematode genus abundance and biomass data to test the impact of MPs on community structure, based on a Bray–Curtis similarity matrix. Data were fourth-root transformed to down-weight the influence of hyper-abundant taxa and to balance the contribution of rare species. Non-metric multidimensional scaling (nMDS) ordination was used to visualize patterns in community structure. A two-way permutational multivariate analysis of variance (PERMANOVA) was subsequently used to test for significant differences in community composition. The statistical model included 'Treatment' (four levels: Control, 10^3, 10^5, 10^7 particles/mL) and 'Time' (three or two levels, depending on the experiment) as fixed factors, along with their interaction term. When significant differences were found, pair-wise tests were conducted: for these comparisons, p-values were obtained from Monte Carlo simulations when the number of unique permutations was low. The genera contributing to differences in community composition were identified using a similarity percentage (SIMPER) analysis. The assumption of homogeneous multivariate dispersion was tested using PERMDISP to ensure that significant PERMANOVA results reflected shifts in community composition rather than differences in within-group variability.

Total nematode density, genus richness (S) and Shannon–Wiener diversity (H') were calculated as a robust measure of overall diversity that accounts for both richness and evenness, and to specifically isolate changes in the dominance structure of the community. Pielou's evenness (J'), community biomass, and the functional indices (MI and TDI) were also analyzed. To test for significant effects of 'Treatment' and 'Time' on these metrics, a two-way PERMANOVA based on a Euclidean distance matrix of the normalized data was employed.

To assess ingestion dynamics, the influence of 'Treatment', 'Time' and 'regions' on the gut load of MPs was evaluated using the same PERMANOVA design on the ingested MP data. To explicitly link community structure and functional diversity to MP sequestration, correlation analyses (Spearman's rank) were performed to relate the average ingestion rate within specific functional groups (e.g., trophic groups 1B, 2A; c-p group 2) and diversity indices (total nematode density, genus richness, Shannon–Wiener diversity, Pielou's evenness) to their defining traits. This analysis also identified the primary biological vectors for MP entry into the food web. Furthermore, to evaluate the consequences of ingestion on community biomass (Hypothesis H3), the relationship between the MP gut load on the one hand and total community biomass or individual biomass on the other was assessed using Spearman's rank correlation.

All statistical analyses were conducted using PRIMER 7 (with the PERMANOVA + add-on) and STATISTICA 7, with a significance level (α) of 0.05. These software packages, in conjunction with Sigmaplot 12.5, were used to generate all graphical representations.

Fig. 1 Temporal and morphospatial distribution of ingested microplastics within nematodes. Heatmap illustrating the average quantity of 1-µm polystyrene microspheres in distinct body regions (pharyngeal, anterior intestine, posterior intestine) over the course of the short-term (T3, T6, T9) and long-term (T15, T30) experiments. Each column represents a sampling time point, and each row represents a body region. The color intensity, from white (low) to black (high), corresponds to the total number of particles, as indicated by the scale bar (0–1000 particles). Data shown are exclusively from the highest density treatment (10^7 particles/mL), as no ingestion was detected in the lower density or control groups

3 Results

3.1 MP sequestration capacity of the nematode community during short- and long-term exposure

3.1.1 Short-term exposure

Nematodes readily ingested 1-µm MP microspheres in the short-term experiment (Fig. S1). However, ingestion was treatment-dependent (Pseudo-F = 386.68; p = 0.0001; PERMDISP = 0.0001), with uptake observed exclusively in the highest density treatment (10^7 particles/mL) (p = 0.001), where a total of 4452 particles were quantified across 13 distinct genera. Within this treatment, the MP burden increased significantly over time (Pseudo-F = 4.508; p = 0.023; PERMDISP = 0.623), nearly doubling from the third to the ninth day of exposure (294 ± 164 vs. 581 ± 281 particles; p = 0.003).

The distribution of the particles also varied significantly among gut regions (Pseudo-F = 102.3; p = 0.0001; PERMDISP = 0.0002). The pharyngeal region of the nematodes contained significantly fewer MPs (30.33 ± 4.81 particles; p = 0.001), whereas the majority of particles were found within the intestine, with a substantially greater accumulation in the posterior intestinal region (839.33 ± 127.39 particles) compared to the anterior part (614.33 ± 170.40 particles; p = 0.015). The analysis of the time vs. body region interaction (Fig. 1) revealed that the MP load in the pharyngeal region remained low and constant throughout the nine days (ranging from 5.25 ± 1.4 to 8.25 ± 1.24 particles). In contrast, progressive accumulation was observed in both regions of the intestine, with a significantly greater build-up in the posterior region over time (145.25 ± 20.34 and 239.75 ± 29.71 particles) compared to the anterior region (69 ± 20.34 and 187.75 ± 20.95 particles, respectively) (p < 0.025).

MP uptake was not homogeneous across the community, rather, it was concentrated in a few key taxa. Although 13 of the 52 genera identified in the short-term experiment ingested microspheres, the genus *Daptonema*, representing over 87% of the community's relative abundance, accounted for 89.9% (3998 particles) of the total

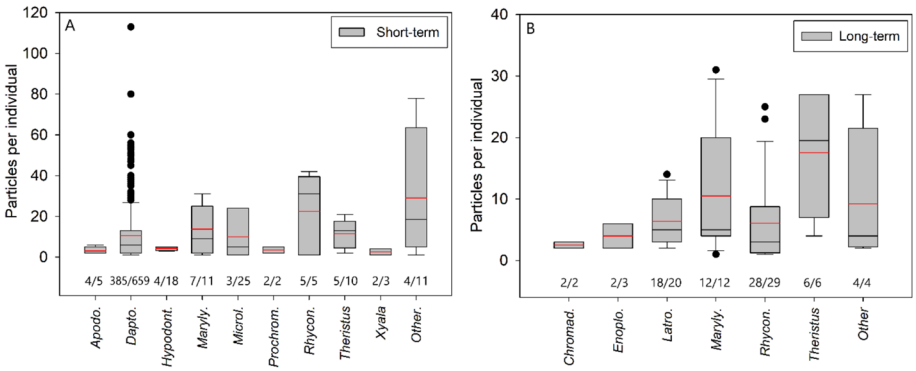

Fig. 2 The figure illustrates the distribution of the number of ingested particles per individual for each nematode genus where ingestion was detected. The left panel displays data from the short-term (9-day) experiment, and the right panel displays data from the long-term (30-day) experiment. Data are shown exclusively from the highest concentration treatment (10^7 particles/mL). The boxplots represent the distribution of particle counts only among the individuals that ingested MPs. Each boxplot shows the median (central black line) and mean (red line). Outliers are plotted as individual black dots. The fractions below each genus label indicate the prevalence of ingestion within the subsample analyzed for each replicate. This subsample consisted of up to the first 100 identified nematodes per replicate, as described in the methods. The fraction is formatted as (number of individuals with ingested particles / total number of individuals of that genus within the assessed subsample). The 'Other' category aggregates several genera that were present at low abundances and showed minimal ingestion. All data are based on n = 4 replicates

community ingestion, with an average of ~ 10.0 particles per individual (Fig. 2A). The genera *Rhynchonema* (112 particles, avg. ~ 22 particles/individual), *Marylynnia* (96 particles, avg. ~ 14 particles/individual), *Viscosia* (78 particles), and *Theristus* (59 particles, avg. ~ 12 particles/individual) collectively accounted for 8% of the uptake, while 8 further genera collectively contributed less than 3% of the total ingestion, highlighting a pattern of functional dominance rather than a generalized community response. Across all exposure times, *Daptonema* was the genus that contributed most to this similarity (> 85%). The second genus to most consistently ingest MPs across replicates was *Theristus* (8.53%) after three days, *Hypodontolaimus* (6.25%) after six days, and *Marylynnia* (4.75%) after nine days.

3.1.2 Long-term exposure

In the long-term experiment, MP ingestion remained strongly treatment-dependent (Pseudo-F = 37.056; p = 0.0001; PERMDISP = 0.0001) and was also exclusively observed in the highest density treatment (10^7 particles/mL). Notably, the total MP load quantified over the 30-day period was substantially lower than that observed in the short-term experiment, with a total of only 571 particles distributed across ten genera. The duration of exposure did not influence the quantity of ingested particles ($p > 0.05$; Fig. 1), although gut loads of MPs tended to increase with time. The distribution of particles across gut regions showed significant differences (Pseudo-F = 44.197; p = 0.0001; PERMDISP = 0.111) between the pharyngeal region of the nematodes and both intestinal regions ($p < 0.001$). However, in contrast to the short-term experiment, there was no significant difference in particle accumulation between the anterior and posterior intestine (85.5 ± 11.03 and 184.5 ± 54.36 particles, respectively).

Long-term exposure altered the pattern of functional dominance in MP ingestion. Instead of a single dominant taxon, the sequestration function was shared among four key genera: *Rhynchonema* (170 particles; 29.8%; avg. ~ 6 particles/individual) (Fig. 2B), *Latronema* (126 particles; 22.1%; avg. ~ 7 particles/individual), *Marylynnia* (120 particles; 21%; avg. 10 particles/individual), and *Theristus* (105 particles; 18.4%; avg. ~ 18 particles/individual). Together, these four genera were responsible for over 91% of all ingested particles. *Gammanema* carried approximately 4.7% (27 particles) of the MPs, while the genera *Enoploides*, *Ascolaimus*, *Chromadorella*, *Viscosia* and *Xyala* contributed a combined total of approximately 4%. SIMPER analysis revealed that T30 exhibited greater within-replicate similarity (56.28%) than T15 (44.79%). At both time points, *Rhynchonema* and *Latronema* were the primary genera contributing to this similarity. However, their relative contributions shifted over time: at 15 days of exposure, *Rhynchonema* contributed 83.68% and *Latronema* only 16.32% to the similarity. By day 30, *Rhynchonema* and *Latronema* contributed more equitably, at 55.32% and 44.68%, respectively.

Despite differences in the community response to MP ingestion patterns, a core group of key taxa for MP sequestration was evident across both temporal scales. Of the 18 genera that ingested MPs, five were present in both experiments. Among these, *Rhynchonema*, *Marylynnia*, and *Theristus* consistently carried MPs in their guts. Across both experiments, the top-five nematode genera carrying the most MPs in their guts comprised non-selective deposit-feeders (feeding type 1B. *Daptonema, Rhynchonema, Theristus*, all belonging to the same family: Xyalidae), predators/omnivores (feeding type 2B: *Latronema, Viscosia, Gammanema*) and one genus of epistrate feeders (2A: *Marylynnia*).

3.2 Effects of MPs on community structure and influence on sequestration

3.2.1 Short-term exposure

Short-term exposure to MPs significantly altered the nematode community structure over time (Pseudo-F = 2.25; p = 0.01; PERMDISP = 0.009), with the genus composition becoming significantly different from the control after nine days of exposure (p = 0.035). The impact was not dose-dependent but varied among treatments (Pseudo-F = 3.027; p = 0.0002; PERMDISP = 0.0005). The most pronounced effects were observed in the lowest-density treatment (10^3 particles/mL), genus composition of which differed significantly from both the experimental control (p = 0.0005) and the highest-density treatment (10^7 particles/mL; p = 0.0032) (Fig. S2). In contrast, communities exposed to intermediate and high MP densities (10^5 and 10^7 particles/mL) did not differ significantly from the control (p = 0.082).

SIMPER analysis revealed that this dynamic was strongly driven by the genus *Daptonema*. The greatest dissimilarities in faunal composition were observed between the 10^7 and 10^3 particles/mL treatments (70.1%) and between the control and 10^3 particles/mL treatments (68.98%). In both cases, the dissimilarity was primarily driven by the reduced abundance of *Daptonema* in the 10^3 particles/mL treatment (Fig. 5). Conversely, the high similarity between the 10^7 particles/mL treatment and the control was maintained by the consistently high contribution of *Daptonema* in both. Among-replicate

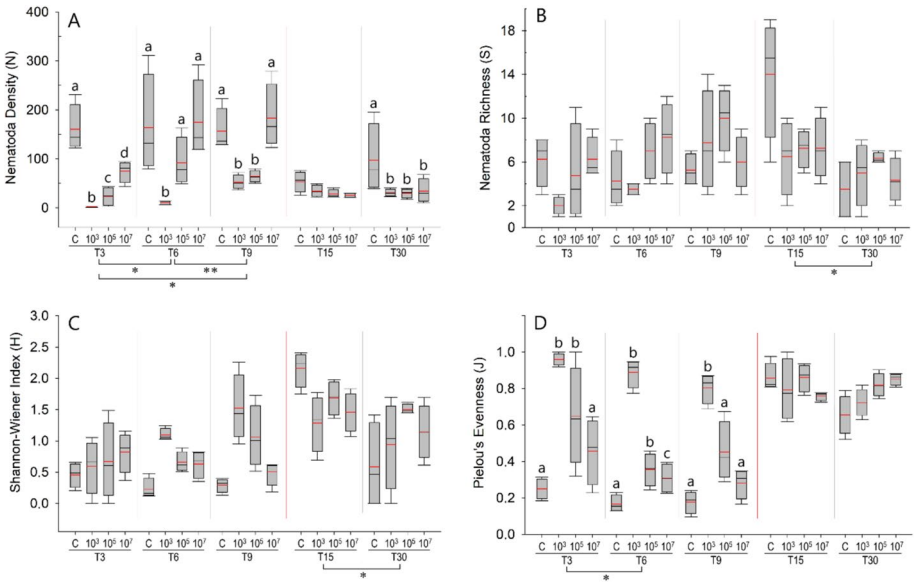

Fig. 3 Temporal dynamics of nematode community structural parameters under different microplastic exposure scenarios. Figure panels illustrate changes in **A** genus richness (S), **B** total nematode density (N; individuals/10 cm^2), **C** Shannon–Wiener diversity (H'), and **D** Pielou's evenness (J') across short-term (T3, T6, T9) and long-term (T15, T30) exposure periods. On the x-axis, 'C' denotes the control group, while 10^3, 10^5, and 10^7 represent the microplastic densities in particles/mL. The boxplots display the median (black line), the mean (red line), the interquartile range (25th–75th percentiles), and the full data range (whiskers). Lowercase letters above the boxes indicate significant differences among treatments at a specific time point, as determined by pair-wise post-hoc tests ($p < 0.05$); treatments not sharing a common letter are significantly different. Asterisks below the time points denote significant temporal differences, where * indicates $p < 0.05$ and ** indicates $p < 0.01$. All data are based on $n = 4$ replicates per treatment group

similarity was highest in the control (54.24%), followed by the 10^7 (48.4%), 10^5 (40.37%), and 10^3 particles/mL (26.79%) treatments. *Daptonema* was the primary genus contributing to this similarity, with its contribution increasing as the density of MPs increased (Fig. 5).

A total of 2509 individuals distributed across 52 distinct genera were identified (Table S1). Nematode density differed significantly among treatments (Pseudo-F = 39.9; $p = 0.0001$; PERMDISP = 0.157), with lower nematode densities at the low and intermediate MP treatments (10^3 and 10^5 particles/mL) compared to the control ($p = 0.006$) and the high MP density treatment (10^7 particles/mL; $p = 0.006$). Nematode density also varied significantly over time within treatments (Pseudo-F = 6.66; $p = 0.0003$). After three days of exposure, the effect was most pronounced, with all treatments differing from each other and from the control ($p = 0.032$), and with nematode density being lowest in the treatment with the lowest MP densities (Fig. 3A). However, a pattern of recovery was observed in the 10^7 particles/mL treatment, where density no longer differed from the control from the sixth day onward. In contrast, the remaining treatments (10^3 and 10^5 particles/mL) continued to exhibit significantly lower densities compared to the control throughout the experiment ($p = 0.006$).

Neither genus richness (S) nor Shannon–Wiener diversity (H') of the nematode community were affected by short-term MP exposure, with no significant effects detected for time, treatment, or the interaction between these factors (Fig. 3B, C; Table S2). In

contrast, evenness (J) of the community was significantly affected by the different MP densities (Pseudo-F = 3.950; p = 0.033; PERMDISP = 0.961). All treatments with MPs exhibited a substantially higher evenness compared to the control (p = 0.002) (Fig. 3D). Community evenness also varied significantly over time (Pseudo-F = 62.859; p = 0.0001; PERMDISP = 0.961). This shift in evenness was directly linked to the response of the dominant genus, *Daptonema*, and so was community abundance. In both the control and the highest MP density treatment (10^7 particles/mL), *Daptonema* maintained a high abundance (over 90% of the community), resulting in a very low community evenness. Conversely, in the low and intermediate MP treatments (10^3 and 10^5 particles/mL, respectively), the absolute and relative abundance of *Daptonema* strongly decreased, particularly in the low-density treatment, where it fell to less than 17% by the third day of exposure and did not exceed 50% throughout the experiment. This reduction in the dominance of *Daptonema* allowed for an increase in the relative abundance of other taxa, resulting in a community with a more homogeneous distribution.

Correlation analysis confirmed that the restructuring of the nematode community under short-term MP exposure had direct consequences for its collective function. The total ingestion capacity of the community was positively correlated with total nematode density (r = 0.65, p < 0.02) (Fig. 5) but negatively correlated with Pielou's evenness (r = -0.58, p < 0.04) (Fig. 5; Table S3), illustrating that the biological sink function was strongly driven by a single taxon rather than by the entire community.

Daptonema was the taxon that most influenced both the structural responses of the community and its MP sequestration capacity. In the low (10^3) and intermediate (10^5) densities, where no uptake was detected, the abundance of *Daptonema* was significantly reduced compared to the control. In contrast, at the highest density (10^7 particles/mL), *Daptonema* demonstrated high persistence, maintaining a density similar to that of the control (Fig. 5). Simultaneously, it functioned as the principal biological sink for MPs, responsible for almost 90% of all ingested particles. A significant positive correlation was observed between the density of *Daptonema* in this treatment and the quantity of ingested particles (r = 0.56, p < 0.05).

3.2.2 Long-term exposure

Long-term exposure to MPs resulted in a significant shift in the temporal dynamics of the nematode community (Pseudo-F = 3.450; p = 0.01; PERMDISP = 0.234), although no significant treatment effect (Pseudo-F = 1.363; p = 0.117; PERMDISP = 0.252) or time vs. treatment interaction (Pseudo-F = 1.094; p = 0.379) was observed. The nMDS ordination revealed distinct groupings for T15 and T30, and Pearson correlation indicated that the vectors corresponding to the dominant nematode genera correlated more positively with T15 than with T30 (p = 0.014) (Fig. S3). SIMPER analysis revealed the drivers of this temporal dynamic. At T15, the community structure was primarily driven by the genera *Rhynchonema* (37.55%) and *Ascolaimus* (11.49%), which were the main contributors to within-treatment similarity at this time-point (40.37%). By T30, however, the community had restructured; the density of *Ascolaimus* diminished (as did the genera *Latronema*, *Rhynchonema*, *Bathylaimus*, *Marylynnia*, and *Chromadorella*), and the

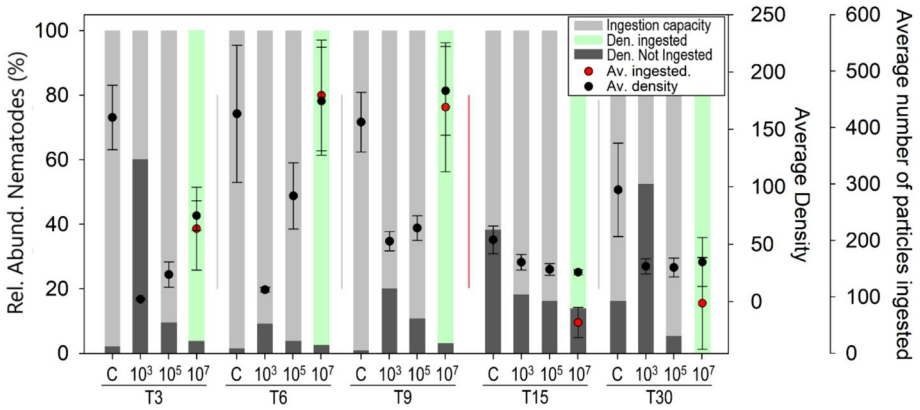

Fig. 4 Relationship between community composition by ingestion status, total nematode density, and ingestion magnitude. The stacked bars represent the relative abundance (%) of the nematode community, partitioned by ingestion status (primary left y-axis): the green portion shows the abundance of genera with detected ingestion in a given treatment; the dark grey portion shows the abundance of non-ingesting genera; and the light grey portion represents the "ingestion capacity"—the abundance of genera that can ingest but did not under that specific condition. Overlaid on the bars are the mean nematode density (black circles; middle y-axis, individuals/10 cm^2) and the mean number of particles ingested per individual (red circles; right y-axis). Error bars indicate standard deviation. The x-axis displays the control (C) and MP densities across short-term (T3, T6, T9) and long-term (T15, T30) exposure. Note that green bars and red points are present only in the 10^7 particles/mL treatment, as this was the sole condition where ingestion occurred. All data are based on n = 4 replicates

genus *Latronema* emerged as the second most abundant (31.99%) after *Rhynchonema* (32.33%). Together, these two genera were the primary contributors to similarity at T30 (30.42%).

A total of 693 individuals from 37 distinct genera were identified across the long-term experiment (Table S4). The different densities of MPs significantly affected nematode density (Pseudo-F = 5.404; p = 0.006; PERMDISP = 0.446), which was consistently lower in all MP-exposed treatments compared to the control ($p < 0.04$) (Fig. 3A). In contrast, diversity indices were not impacted by treatment (Table S5). However, both genus richness (Pseudo-F = 16.307; p = 0.003; PERMDISP = 0.285) and Shannon–Wiener diversity (Pseudo-F = 16.307; p = 0.0036; PERMDISP = 0.285) varied drastically with time (Pseudo-F = 5.734; p = 0.038; PERMDISP = 0.0002). This temporal effect was characterized by a substantial reduction in biodiversity, with the community losing 16 of the 37 identified genera by day 30 (p = 0.003) (Fig. 3B). With the exception of *Ascolaimus* and *Daptonema*, which disappeared from all MP treatments but persisted in the control, all other genera disappeared from both the control and treatment microcosms between T15 and T30. A significant time × treatment interaction was detected for Pielou's evenness (J') (Pseudo-F = 5.618; p = 0.027). This difference was driven by a shift in dominant taxa in 30 days: whereas the control was dominated by *Chromadorella* (53.8%), the community exposed to the highest MP density was co-dominated by a consortium of *Rhynchonema*, *Latronema*, and *Theristus* (contributing 28%, 20%, and 20%, respectively) (Table S5).

In stark contrast to the short-term observations, the analysis of the long-term experiment revealed a decoupling between community structure and the MP sequestration function (Fig. 4, 5). None of the community structure metrics, including density (r = 0.57, p = 0.18), genus richness (r = 0.50, p = 0.24), Shannon–Wiener diversity

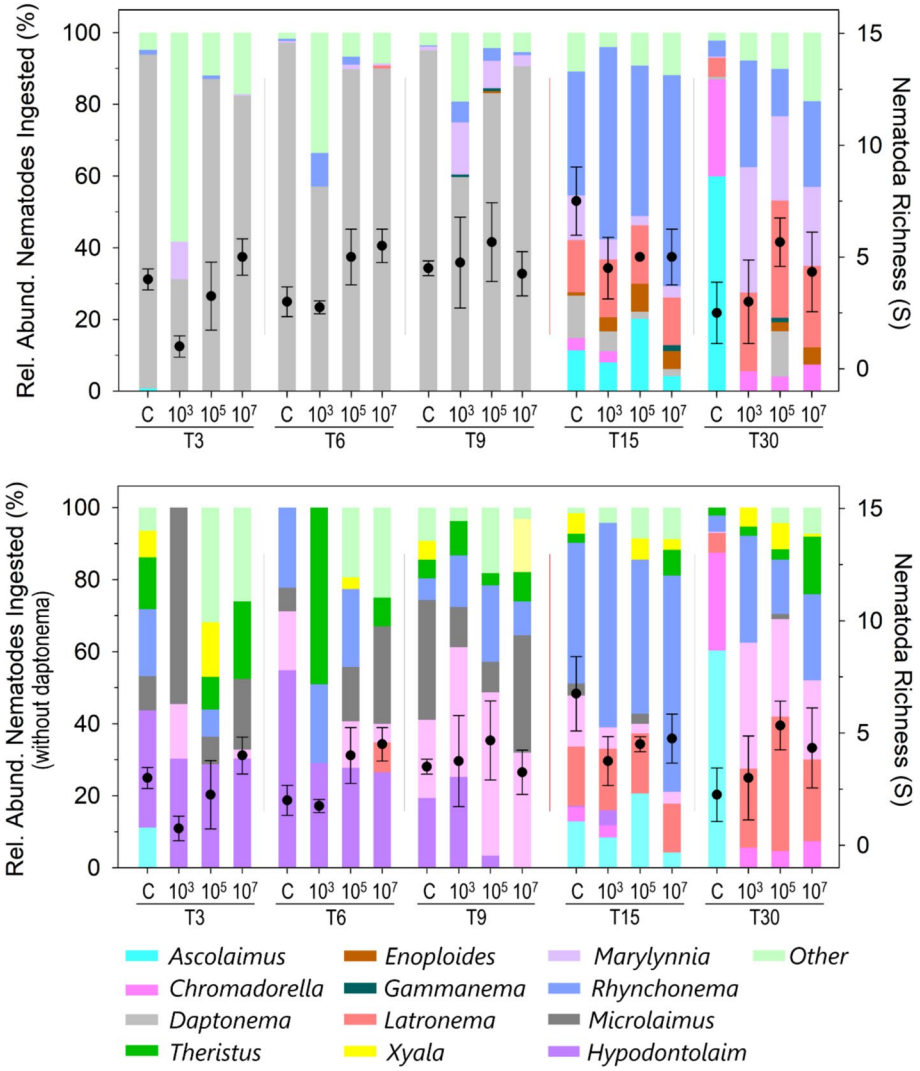

Fig. 5 Composition and richness of the MP-ingesting nematode assemblage. The figure illustrates the temporal dynamics of the nematode genera capable of ingesting MPs, focusing exclusively on the subset of taxa in which ingestion was detected at least once during the experiments. The stacked bars represent the relative abundance (%) of these specific genera (left y-axis), and the overlaid points (black circles) show their corresponding mean genus richness (S) (right y-axis), with error bars indicating the standard deviation. Therefore, in the 10^7 particles/mL treatment, the bars represent the composition of the actual ingesting community. In the control, 10^3, and 10^5 particles/mL treatments (where no ingestion was observed), the bars represent the composition and richness of the potential ingesting assemblage, showing how this functional group was structured in the absence of uptake. To better visualize the community structure beyond the dominant taxon, the data is presented in two panels: the Top Panel shows the full composition of this assemblage, highlighting the overwhelming dominance of *Daptonema* in the short-term, while the Bottom Panel displays the same data with *Daptonema* excluded to reveal the proportional shifts among the sub-dominant ingesting genera. The x-axis displays the control (C) and the three MP concentrations across the experimental time points (T3 to T30). All data are based on n = 4 replicates per treatment group

(r = −0.50, p = 0.25), and evenness (r = −0.14, p = 0.75), showed a significant correlation with the total density of MPs ingested by the community (p > 0.05 for all). Furthermore, the densities of the individual genera that ingested microspheres also did not correlate with the number of particles recorded in the nematode guts (Table S6-S7).

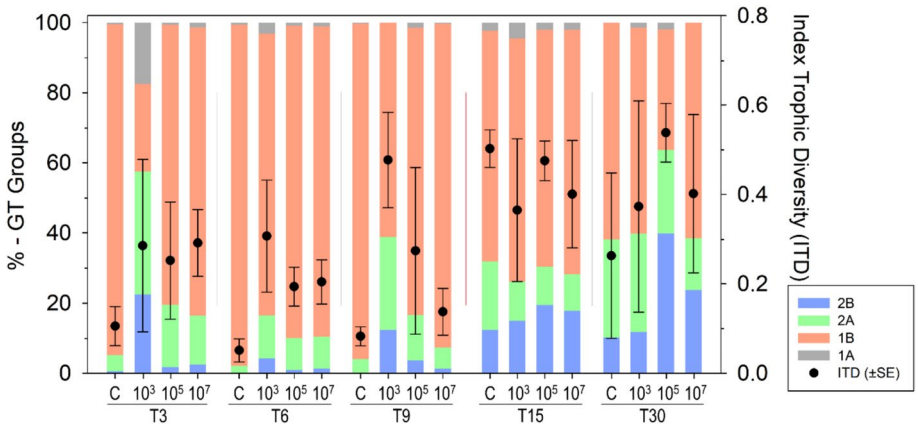

Fig. 6 Temporal dynamics of nematode trophic group composition and trophic diversity (estimated by the Trophic Diversity Index, TDI). The stacked bars represent the relative abundance (%) of each trophic group (GT) within the nematode community (left y-axis). Black circles represent the mean TDI of the community (right y-axis), with error bars indicating the standard error (SE). Trophic groups are abbreviated as follows: 1A = selective deposit-feeders; 1B = non-selective deposit-feeders; 2A = epistrate-feeders; 2B = predators/omnivores. The x-axis displays the control (C) and the three MP densities treatments (10^3, 10^5, 10^7 particles/mL) across the experimental time points (T3 to T30, time in days). All data are based on n = 4 replicates per treatment group

3.3 Functional diversity as a predictor of ingestion, and identification of key MP vectors

3.3.1 Short-term exposure

The functional structure of the nematode community, considering both trophic groups and life-history strategies, exhibited significant alterations in response to short-term MP exposure. Regarding the trophic structure, all four feeding groups were present, but their distributions differed significantly among treatments (Pseudo-F = 10.364; p = 0.0001), over time (Pseudo-F = 3.71; p < 0.001), and in the interaction of these factors (Pseudo-F = 3.9844; p = 0.0001). Among the groups, non-selective deposit-feeders (1B) were the most abundant and showed significant variations across all analyzed factors ($p \leq 0.02$). In contrast, selective deposit-feeders (1A) did not differ significantly either by time or by treatment, remaining the least abundant group throughout the study (Fig. 6). SIMPER analysis revealed that the differences in trophic group composition in time were strongly driven by non-selective deposit-feeders (1B) and epistrate feeders (2A). The latter was the second most abundant trophic group, varying significantly among treatments (Pseudo-F = 3.959; p = 0.01). Together, 1B and 2A dominated the nematode communities across most treatments and times, with a combined contribution of 88%–98%. An exception was observed in the lowest-MP density treatment (10^3 particles/mL) after three days, where their joint contribution was approximately 60% (Fig. 6), and predators/omnivores (2B) increased in relative abundance. Predatory/omnivore nematodes (2B), in turn, varied significantly across time (Pseudo-F = 4.416; p = 0.01), independently of MP exposure. The Trophic Diversity Index (TDI) reflected these structural shifts, differing significantly among treatments (Pseudo-F = 6.8; p < 0.01). The MP-exposed treatments showed higher trophic diversity compared to the control ($p \leq 0.05$), particularly in the

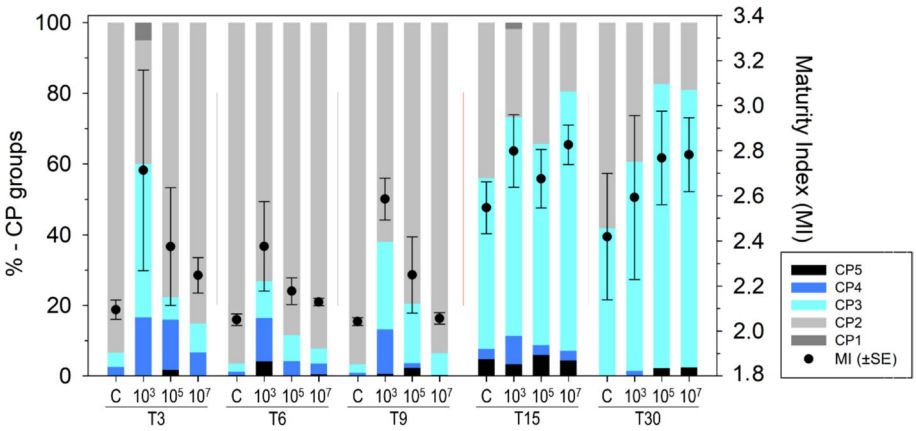

Fig. 7 Temporal dynamics of nematode life-history (c-p) group composition. The stacked bars represent the relative abundance (%) of each colonizer-persister (c-p) group within the nematode community (left y-axis). Overlaid points (black circles) represent the mean Maturity Index (MI) of the community (right y-axis), with error bars indicating the standard error (SE). The x-axis displays the control (C) and the three MP density treatments (10^3, 10^5, 10^7 particles/mL) across the experimental time points (T3 to T30). All data are based on n = 4 replicates per treatment group

10^3 particles/mL treatment, which exhibited a trend of increasing trophic diversity over time (Fig. 6).

Community composition based on life-history groups varied significantly over time (Pseudo-F = 3.989; p = 0.001), treatment (Pseudo-F = 9.876; p < 0.0001), and their interaction (Pseudo-F = 4.448; p = 0.0001). SIMPER analysis revealed that the differences were strongly driven by c-p 2 (78–96%), which was the most abundant group, showing significant variations across all factors (p < 0.01). The second-most abundant group was c-p 3, which contributed mostly to differences in time (Pseudo-F = 4.588; p = 0.01). Nematodes with c-p 4 also differed across treatment vs. time (interaction: Pseudo-F = 4.065; p = 0.005). Notably, the control differed from the lower density treatments by the greater presence of cp-2 groups ($p \leq 0.01$). Among the MP-exposed treatments, a trend was observed of increasing proportions of nematodes belonging to c-p 3 and c-p 4 and a reduction in c-p 2 as MP density increased ($p \leq 0.02$). This trend persisted over time, with an increase between T3 and T9 (Fig. 7). Corroborating these patterns, the analysis of the Maturity Index (MI) also revealed significant alterations in response to MP exposure among treatments (Pseudo-F = 4.9032; p < 0.01), following a trend similar to that observed for the c-p values, with MI values decreasing as MP density increased (10^3–10^7 particles/mL; p = 0.05) (Fig. 7).

Correlation analyses between MP gut load of nematodes and the functional indices revealed a clear pattern of taxonomic dominance and functional selectivity. Among life-history strategies, c-p 2 was dominant throughout most of the experiment and was responsible for approximately 80–90% of the total ingestion over time (r = 0.65, p = 0.02). Among trophic groups, non-selective deposit-feeders (1B) were the main MP sequestrators, showing a positive correlation with gut load (r = 0.67, p = 0.01). They were followed by epistrate feeders (2A) and predators/omnivores (2B), whereas selective deposit-feeders (1A) exhibited minimal to no ingestion. Over time, the 1B group maintained the largest proportion of MP uptake, while the 2A and 2B groups made smaller and more

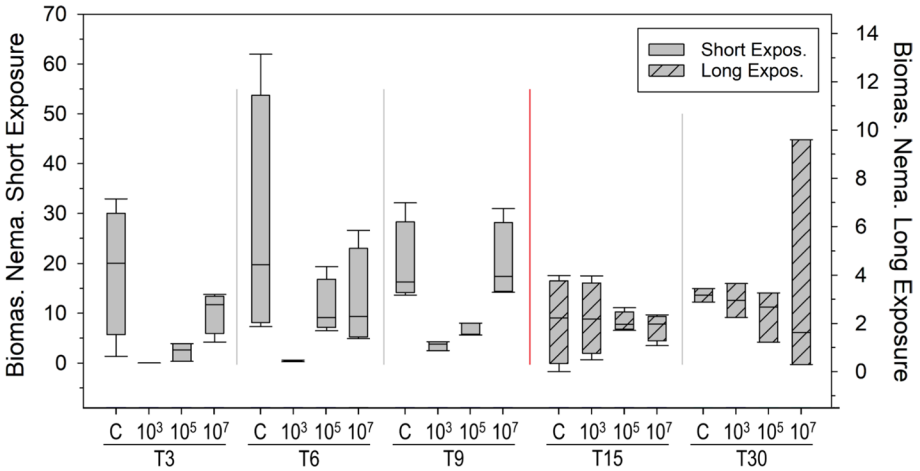

Fig. 8 Total nematode biomass across short- and long-term microplastic exposure experiments. The boxplots show the total community biomass (µg wet weight/10 cm^2) in the different experimental treatments. Data from the short-term exposure (T3, T6, T9; solid grey bars) are plotted against the primary left y-axis. Data from the long-term exposure (T15, T30; hatched bars) are plotted against the secondary right y-axis. On the x-axis, 'C' denotes the control group, while 10^3, 10^5, and 10^7 represent the microplastic densities in particles/mL. The boxplots display the median (black line), the interquartile range (25th–75th percentiles), and the full data range (whiskers). All data are based on n = 4 replicates per treatment group

variable contributions. At the genus level, *Daptonema* (c-p 2; 1B) emerged as the principal vector, responsible for approximately 90% of all ingested particles. Other genera, such as *Rhynchonema* (1B; c-p 3), and *Apodontium*, *Hypodontolaimus*, *Karkinochromadora*, *Perepsilonema*, *Marylynnia*, and *Viscosia* (2A-2B; c-p 3–4), contributed only minor proportions, confirming that the MP ingestion function was concentrated in a few taxa within the dominant categories.

3.3.2 Long-term exposure

The functional structure of the nematode community did not exhibit statistically significant differences among MP treatments or times in the long term. The four trophic groups were recorded in all treatments, with non-selective deposit-feeders (1B) being the most prominent, as in the short-term experiment. However, this time their contribution was smaller (60–70%) except in the 10^5 particles/mL treatment at T30, where it dropped sharply to ~ 35% (Fig. 6). A non-significant trend of reduced 1B abundance over time was observed (Fig. 6). This decline was accompanied by an increase in the relative abundance of epistrate feeders (2A) and predators/omnivores (2B). In this scenario, the 2B group became the second most abundant, followed by 2A, while selective deposit-feeders (1A) remained the least abundant group throughout the experiment (Fig. 6). The TDI showed higher values in the long term compared to the short term, but this difference was not statistically significant.

The long-term patterns of life-history strategies also differed from those observed in the short term. Instead of a predominance of c-p 2, the c-p 3 class became dominant, with contributions varying from approximately 50% to 80% (Fig. 7). The only exception occurred in the control at T30, where c-p 2 surpassed c-p 3, representing 58% of the community versus 42%, respectively. At T15 there was a greater participation of less

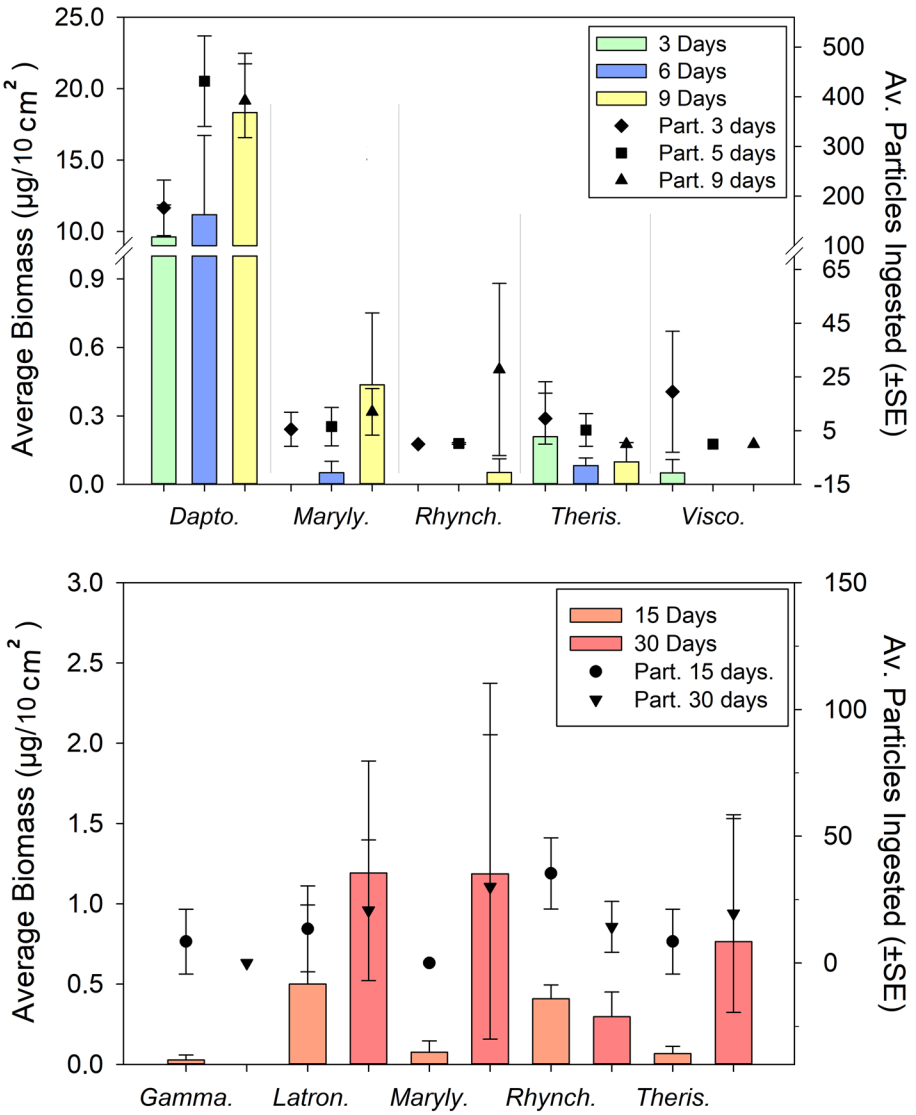

Fig. 9 Temporal shift in the relationship between genus-specific biomass and microplastic ingestion. The panels compare the average biomass (bars; left y-axis) and the average number of ingested particles (points; right y-axis) for the key ingesting genera in the (Top Panel) short-term (3, 6, and 9 days) and (Bottom Panel) long-term (15 and 30 days) experiments. Error bars indicate the standard error (SE). The top panel highlights the dominance of *Daptonema* in both biomass and ingestion during the initial exposure. The bottom panel demonstrates the loss of *Daptonema* as a functional vector in MP-exposed treatments and the emergence of a functionally diverse consortium (*Latronema*, *Marylynnia*, *Rhynchonema*, *Theristus*) that collectively contributes to both community biomass and MP sequestration under chronic exposure. Note the significant difference in the scales of both y-axes between the panels

common c-p groups such as c-p 4, the abundance of which was strongly reduced by T30 (Pseudo-F = 8.08; $p < 0.006$) (Fig. 7).

3.4 Consequences of MP ingestion on community biomass

3.4.1 Short-term exposure

Total nematode community biomass in the short-term experiment exhibited a pattern similar to that observed for density. Specifically, treatment significantly affected community biomass (Pseudo-F = 3.6476; p = 0.03; PERMDISP = 0.02), but time and the interaction of treatment vs. time did not. Exposure to the lowest MP densities (10^3 particles/mL) resulted in lower nematode biomass compared to the experimental control (p = 0.04) and to the other MP treatments (p < 0.015) (Fig. 8). Notably, the biomass in the intermediate (10^5 particles/mL) and high (10^7 particles/mL) density treatments did not differ significantly from the control (p > 0.39).

In contrast, the composition of biomass by genera differed significantly over time (Pseudo-F = 2.239; p = 0.006; PERMDISP = 0.222) and among treatments (Pseudo-F = 2.978; p = 0.0006; PERMDISP = 0.036). Once again, *Daptonema* was the primary driver of this response, especially in the 10^3 particles/mL treatment. The average biomass for genus *Daptonema* in the low-density treatment ranged from 0.22–2.04 µg/10 cm² over time, whereas in the control, it ranged from 16.73–26.94 µg/10 cm², explaining the high dissimilarity observed between these two treatments (69.07%). Conversely, in the highest density treatment (10^7 particles/mL), *Daptonema* not only maintained a high biomass (ranging from 9.62–18.32 µg/10 cm²), similar to the control, but was also the genus with individual biomass being strongly positively correlated with the number of ingested MP particles (r = 0.71, p < 0.009) (Fig. 9A).

3.4.2 Long-term exposure

Long-term exposure to MPs did not alter the total nematode biomass over time (Pseudo-F = 0.337; p = 0.654; PERMDISP = 0.26), by treatment (Pseudo-F = 0.333; p = 0.829; PERMDISP = 0.642), or in interaction (Pseudo-F = 0.282; p = 0.895). However, the composition of biomass by genera differed significantly over time (Pseudo-F = 3.528; p = 0.002; PERMDISP = 0.009), with the total biomass being substantially higher after 30 days of exposure (p = 0.007) (Fig. 8). SIMPER analysis indicated that this change was driven by an increase in the biomass of the genera *Latronema* and *Marylynnia* (Fig. 9B), which together accounted for 63% of the dissimilarity between the two time points. Although no correlation was found between the biomass of these specific genera and MP ingestion (p > 0.05), a significant positive correlation was found between the total community biomass and the total number of ingested particles (r = 0.78, p < 0.03). This result indicates that the sequestration function in the long term is linked to the total biological mass of the community rather than to a single taxon.

4 Discussion

Although benthic sediments are recognized as a principal sink for the 'missing plastic' [2, 12], the biological processes that govern the fate of microplastics (MPs) within this vast reservoir, and the role of the associated biota, remain largely unexplored and

underestimated. The role of nematodes in particular, the highly abundant and functionally diverse small metazoans in marine sediments [18, 19], represents a fundamental gap in our understanding of the plastic cycle. A key discovery of our study is the decoupling of the sequestration function from direct ecological harm. Specifically, the sequestration function is dominated by opportunistic taxa and occurred only at the highest MP density. Crucially, the most severe adverse effects on the community, such as reduced density and biomass, occurred at the lower and intermediate densities, where no ingestion was detected.

4.1 Effects of MPs on community structure and influence on sequestration

Our findings reveal that the nematode MP sequestration function only becomes apparent under conditions of high contamination, well beyond most currently recorded MP loads in marine sediments (but note that such levels may already be found in highly polluted coastal sediments near urban and industrial zones [46, 47]). This may result from a particle density-dependent ingestion threshold, consistent with previous observations [22, 23, 26]. The explanation for this threshold lies in the complexity of the natural sediment matrix, which effectively reduces the encounter rate between organisms and microspheres. A simple linear extrapolation supports this interpretation: based on the ingestion rate of the dominant (*Daptonema*) in the short-term 10^7 particles/mL treatment, the theoretical ingestion at 10^3 particles/mL would be less than 0.4 particles per individual. Similarly, in the long-term experiment, the predicted uptake would be as low as ~ 0.02 particles. Such low encounter probabilities make detectable ingestion a highly improbable event, framing the observed 'threshold' as a practical detection limit. This is strongly supported by the contrast with simplified systems: while ingestion in our natural sediment occurred only at 10^7 particles/mL, other studies using artificial substrates detected ingestion at much lower densities [26].

Beyond the MP density threshold, the temporal dynamics of ingestion also revealed distinct patterns between the acute and chronic exposures. In the short term, the quantity of ingested MPs progressively increased, nearly doubling between the third and ninth day, which aligns with other short-term studies showing a temporal accumulation of particles [22, 26, 48, 49]. To provide a more direct comparison of sequestration activity over time, we analyzed the ingestion loads within the core genera present in both experiments. In the short-term experiment, *Rhynchonema*, *Marylynnia*, and *Theristus* ingested a total of 112, 96, and 59 particles, respectively. In the long-term experiment, these same genera ingested 170, 120, and 105 particles, respectively (see Supplementary Table S1-4). Although an increase in the number of ingested particles was observed, this change was not substantial for at least two of the three genera. This is consistent with the rapid ingestion and egestion rates of nematodes. Studies have demonstrated that microsphere ingestion can occur in minutes [35], and the particles can be rapidly egested and potentially re-ingested, thereby establishing a dynamic equilibrium rather than indefinite accumulation [35, 50]. Regardless of the temporal scale, the preferential location of particles within the digestive tract was consistent. In alignment with literature for both marine and freshwater nematodes [22, 51, 52], we observed that

a majority of microspheres accumulated in the posterior intestinal region, confirming it as the principal site of retention and transit for MPs.

Given the absence of any substantial particle uptake at all but the highest MP density, our short-term results reveal a counter-intuitive pattern: the most severe community-level impacts occurred in the low and intermediate MP density treatments (10^3 and 10^5 particles/mL). This aligns with previous findings for the broader meiofauna community [22]. One hypothesis is that low MP densities induce a behavioral avoidance response, leading to metabolic exhaustion [53, 54]. Such a response is consistent with hormesis, an ecotoxicological phenomenon documented for MPs at both the population and community level [33, 55], where low densities can trigger a more pronounced stress response than higher ones, which may in turn stimulate compensatory adaptations [56]. Alternatively, adverse effects may be mediated by direct physical contact. The mere presence of MPs can induce adverse effects; for instance, exposure to polystyrene microspheres has been shown to inhibit nematode reproduction even without detectable ingestion [57]. However, it is difficult to reconcile this hypothesis with the absence of significant adverse effects at much higher MP densities and hence also much higher encounter rates.

The long-term community dynamics presented a response pattern distinct from that observed in the short term. Chronic exposure to MPs resulted in a consistent decrease in nematode density. The community's dominance structure was also altered, albeit transiently. In contrast to some studies [33, 58, 59], we observed a significant difference in evenness at T15, where the dominance of *Chromadorella* in the control was replaced by a co-dominant consortium of *Rhynchonema*, *Latronema*, and *Theristus* in the 10^7 particles/mL treatment. The persistence of *Theristus* is at odds with another study [58], which found this genus to be quite sensitive to MPs. However, this difference in evenness did not persist and was likely a consequence of experimental bottling effects, as demonstrated by a dramatic decrease in all diversity measures in the control, with the community losing 16 of the 37 genera between T15 and T30. This shift in taxonomic composition led to a reconfiguration of the principal functional actors involved in MP sequestration, as discussed below. Given that it was not mirrored by a similar impact on the nematode communities in the MP treatments, but rather levelled the initially higher control diversity with that in the MP treatments, this suggests that MP addition did affect nematode communities during the first 15 days of the experiment and mainly eliminated taxa that can be classified as 'broadly sensitive' to various disturbances. Remarkably, though, nematode abundances in the controls did remain significantly higher than in MP treatments, suggesting some compensatory dynamics where the removal of a number of taxa reduced competitive interactions, leading to an increased reproduction of tolerant taxa. This is further supported by the fact that biomass did not follow the abundance trend, pointing to a higher proportion of smaller individuals, for instance juveniles [60].

4.2 Functional diversity: the shifting identity of MP vectors

The results of our short-term experiment reveal that the sequestration function was governed by a single functional type, mainly represented by the highly abundant genus *Daptonema*, but also by *Rhynchonema* and *Theristus*, both members of the same nematode

family, Xyalidae. These exhibited a dual and paradoxical role. At the lower and intermediate MP densities (10^3 and 10^5 particles/mL), the sensitive response of *Daptonema* led to a drastic reduction in density, which, in turn, increased the community's evenness. In stark contrast, at the highest MP density, *Daptonema* demonstrated high persistence and functioned as the principal MP vector, responsible for nearly 90% of all MP ingestion. Indeed, the total sequestration capacity was positively associated with the density of *Daptonema* and negatively with evenness. This finding is perfectly consistent with the known ecology of *Daptonema*. As a non-selective deposit-feeder (1B) and an opportunist (c-p 2), it is functionally predisposed to a fairly non-selective particle ingestion in patches with high abundances of suitable food (mainly protists and/or bacteria) [61] and is known for its tolerance to various disturbances and adverse conditions [21, 62–64]. Corroborating our result, Corinaldesi et al. (2022) also identified *Daptonema* (1B) as the main MP sequestrator after 72 h of exposure. However, in their study, high ingestion was accompanied by a decrease in abundance compared to the control, whereas in our 10^7 particles/mL treatment, the abundance of *Daptonema* remained high. Possible reasons for its sensitivity to lower MP densities in the present study are discussed under 4.1.

In stark contrast, chronic MP exposure triggered a process of functional ecological shifts, altering the identity of the principal ingestion vectors. In the following, it is important to note that the community composition at the start of the long-term experiment differed substantially from that of the short-term experiment, for instance in the near-absence of *Daptonema*, by far the most abundant genus in the short-term trials. Direct comparisons between both experiments therefore warrant due caution. Given the near-absence of *Daptonema*, the sequestration function in the long-term experiment was not dominated by a single genus but was instead shared among a consortium of taxa: *Rhynchonema*, *Marylynnia, Latronema*, and *Theristus*. This group assumed the role of the primary MP sequestrators. This transition of actors reflects a fundamental shift in the dominant functional diversity. While the acute response was driven by an opportunist (c-p 2), the chronic response was characterized by genera with more persistent life-history strategies (c-p 3). Furthermore, the trophic diversity of the MP sequestrators increased, with the inclusion of predators/omnivores (2B; *Latronema*) and epistrate-feeders (2A; *Marylynnia*), albeit with a feeding strategy that is very similar to that of non-selective deposit-feeders (1B) [65]. The trophic response appears to be temporally dependent, with an increase of 1B in some exposures [26] and of 2B in longer exposures [33, 58], as observed here. Regardless of the taxon, a fundamental limiting factor appears to be buccal cavity morphology. The absence of ingestion in selective deposit-feeders (1A) and to a large extent also in (small-bodied) epistrate-feeders (2A) in our study, and the ingestion only by genera with larger buccal cavities (typically ≥ 5 µm) [66–69], corroborate, the findings of Fueser et al. (2019). That study demonstrated that ingestion of MPs is only possible when the buccal cavity size exceeds the particle diameter by a factor of approximately 1.3, providing a mechanistic constraint that explains the selection of certain functional groups as MP vectors.

Synthesizing the functional response, the short-term experiment supported our second hypothesis (H2): the sequestration function was driven by a dominant genus, *Daptonema*, which combines the traits of an opportunist (c-p 2) and a non-selective deposit-feeder (1B). This functional dominance is quantitatively supported by the

Trophic Diversity Index (TDI) results. The higher TDI in the MP treatments was a direct consequence of the suppression of *Daptonema* at lower densities, which led to a loss of dominance and a more even, functionally diverse community. In contrast, the long-term exposure revealed a functional shift. The sequestration function was no longer monopolized by a single c-p 2 taxon but was shared by a consortium of more persistent (primarily c-p 3) and trophically diverse genera, including predators/omnivores (2B). This shift towards a more mature and functionally diverse community diluted the clear TDI pattern observed in the short-term, resulting in no significant differences among treatments in the long term.

4.3 Nematodes as sequestrators of MP: more than an anecdotal role?

Our study demonstrates a dynamic role of nematodes in MP sequestration. Our findings also provide a mechanistic link between an individual's size and its sequestration capacity. The consistent positive correlation between estimated nematode biomass and the number of ingested particles, both in short- and long-term experiments, suggests that larger individuals are more efficient sequestrators, likely due to higher feeding rates or larger gut volumes. Thus, body size emerges as a key functional trait predicting an organism's contribution to MP fluxes. This establishes nematodes not as a passive sink, but as an active biological compartment that transforms and potentially reintroduces MPs into the food web, a role already documented at other levels of the food chain, such as from copepods to jellyfish in planktonic food webs [70].

The question then is whether this role bears any quantitative significance. Let us make a 'back-of-the-envelope' order-of-magnitude calculation, based on data of the short-term experiment and using following assumptions: (1) Like in nature, nematodes are largely concentrated in the upper 2 cm of the experimental microcosms [17, 20]. Here, we assume that 100% of nematodes are present in that depth layer. (2) Not too dissimilar to the field community used for the short-term experiment, we envisage a community completely dominated by (=all individuals belonging to) the non-selective deposit-feeders with r-selected life histories and body sizes similar to *Daptonema* in our study. (3) All nematodes in the community at any time carry a gut load of ~ 10 MPs, the mean value per individual obtained here after 9 days in the short-term experiment (sum of all three gut zones), and all these nematodes eventually get eaten by higher-order consumers [19, 21]. (4) Finally, we assume a nematode abundance of 1000 ind./10cm^2, which is ca 5 times the abundance in our experiment, but closer to 'typical' abundances in intertidal sediments [18]. Based on these assumptions, this imaginary but realistic community would, in a sediment volume of 20 ml containing 10^7 MPs/ml, in total transfer 1.10×10^4 MPs to higher trophic levels upon a total sediment load of 2×10^8 MPs. This is less than 1% of the sediment MP load and hence of very limited quantitative significance in terms of trophic transfer. Furthermore, the observed community biomass patterns support this complex, context-dependent role: biomass was reduced by sublethal stress in the absence of ingestion (short-term, low-density MP), remained resilient under high ingestion by a specialist (short-term, high-density MP), and was maintained through compensatory dynamics despite a chronic loss of density and richness (long-term).

We should be careful, though, not to overgeneralize from this estimate. First, it holds at a very high and not yet commonly occurring MP density. While our data strongly suggests that lower MP densities do not trigger uptake by nematodes, more work is needed to support this conclusion. It holds if there is indeed a minimum threshold density below which no uptake occurs. However, the absence of MP particles in nematode guts as observed here, could also have other explanations. For instance, if we assume a linear dose-dependent storage of particles in nematode guts, the expected number of particles at a sediment load of 10^5 and 10^3 MPs would be 4.2 and 0.042, respectively. In other words, gut loads would be close to, or even well below detection limits. Moreover, it is plausible that a large majority of MPs that are ingested pass the gut and are not retained (de França et al., in press) and that particle retention and accumulation in the gut only occur from a certain uptake or gut loading onwards. Finally, the very limited quantitative importance of nematodes in trophic transfer of MPs should not be readily extrapolated to their potential role in the transfer of MP-associated pollutants. The amount of particles in the gut at any given time is by no means indicative of ingestion rates, given that many nematodes have gut passage times in the order of minutes to hours [37]. Hence, the observed gut loads are but a minute fraction of the total amount of MPs which pass nematode guts. If gut enzymes dislodge and/or modify pollutants that are adsorbed to MP surfaces, the cumulative amount of pollutants that enter nematode bodies may well exceed the amount that can be carried by the observed gut loads by one or two orders of magnitude [7].

5 Conclusions

In summary, our study demonstrates that the role of the nematode community as a biological sink for MPs is a dynamic and multifaceted process. The sequestration capacity (H1) is conditional, dependent on a high-contamination threshold. Under acute exposure, this function is dominated by functional characteristics (H2) related to life history (opportunistic, c-p 2), feeding strategy (non-selective ingestion, 1B, and to a lesser extent other nematodes with wide buccal cavities and limited selectivity) and individual nematode size (larger individuals carry more particles inside their guts). We establish the benthos not as a passive sink, but as an active biological compartment that has the potential to transform and reintroduce MPs into the food web. While our microcosm approach has inherent limitations, such as the use of a single polymer type and size, it successfully isolates fundamental mechanisms and lays the foundations for crucial future research. We urge the scientific community to build upon these findings by: (1) validating these temporal patterns in situ, under complex environmental conditions; (2) experimentally exploring the trophic transfer of MPs and its consequences for carbon assimilation in higher-level consumers; and (3) assessing how different polymer types, shapes, and sizes alter these biogeochemical pathways.

6 Declaration of generative AI and AI-assisted technologies in the writing process

During the preparation of this work the author(s) used Deepl AI in order to translate the first draft of the manuscript. After using this tool/service, the content was reviewed and edited by the author(s) and two native English speakers. The author(s) take full responsibility for the content of the published article.

Supplementary Information

The online version contains supplementary material available at https://doi.org/10.1007/s44289-026-00125-5.

Below is the link to the electronic supplementary material.Supplementary Material 1.

Acknowledgements
The authors wish to thank the Laboratory of Invertebrate Cultivation, Marine Meiofauna and Ecotoxicology (LACIMME) for providing the necessary laboratory space and equipment to conduct the experiments. We are grateful to Emanuele Rodrigues Firmino for her assistance with the photographic documentation for the supplementary material. This study was financed in part by the Coordenação de Aperfeiçoamento de Pessoal de Nível Superior—Brasil (CAPES)—Finance Code 001. Finally, we thank our families and friends for their unwavering support.

Author contributions
F.J. L: Conceptualization, Methodology, Formal Analysis, Investigation, Writing—Original Draft, Writing—Review & Editing. R.B.: Conceptualization, Formal Analysis, Visualization, Writing—Review & Editing. D.A.A.: Conceptualization, Formal Analysis, Writing—Original Draft. I.D.: Investigation, Data Curation. G.A.X.: Investigation, Data Curation. M.E.L.: Investigation, Data Curation. G.L.: Conceptualization, Resources. A.V.: Writing—Review & Editing. T.M.: Conceptualization, Formal Analysis, Writing—Review & Editing, Supervision. G.A.P.: Conceptualization, Formal Analysis, Writing—Original Draft, Writing—Review & Editing, Supervision, Project Administration, Funding Acquisition. All authors reviewed and approved the final manuscript.

Funding
Flávia J. L. de França was a recipient of a fellowship from the Brazilian Federal Agency for Support and Evaluation of Graduate Education (CAPES)—Finance Code 001 (grant 88887.939119/2024–00). Giovanni A. P. Dos Santos by the Public Call 09/2019, both from the Pro-Rectory for Research (PROPESQI) at the Federal University of Pernambuco. The funders had no role in study design, data collection and analysis, the decision to publish, or the preparation of the manuscript.

Data availability
The authors declare that the data supporting the findings of this study are available within the paper and its Supplementary Information files. Should any raw data files be needed in another format they are available from the corresponding author upon reasonable request. Source data are provided with this paper.

Declarations

Ethics approval and consent to participate
Not applicable.

Consent for publication
Not applicable.

Competing interests
The authors declare no competing interests.

Received: 30 September 2025 Accepted: 9 February 2026

Published online: 17 March 2026

References

1. Barnes DKA, Galgani F, Thompson RC, Barlaz M. Accumulation and fragmentation of plastic debris in global environments. Philos Trans R Soc Lond B Biol Sci. 2009;364(1526):1985–98.
2. Woodall LC, Sanchez-Vidal A, Canals M, Paterson GLJ, Coppock R, Sleight V, et al. The deep sea is a major sink for microplastic debris. R Soc Open Sci. 2014;1(4):140317.

3. Obbard RW, Sadri S, Wong YQ, Khitun AA, Baker I, Thompson RC. Global warming releases microplastic legacy frozen in Arctic Sea ice. Earths Future. 2014;2(6):315–20.
4. Uddin S, Fowler SW, Uddin MF, Behbehani M, Naji A. A review of microplastic distribution in sediment profiles. Mar Pollut Bull. 2021;163:111973.
5. Geyer R, Jambeck JR, Law KL. Production, use, and fate of all plastics ever made. Sci Adv. 2017;3(7):e1700782.
6. Jambeck JR, Geyer R, Wilcox C, Siegler TR, Perryman M, Andrady A, et al. Plastic waste inputs from land into the ocean. Science. 2015;347(6223):768–71.
7. Amelia TSM, Khalik WMAWM, Ong MC, Shao YT, Pan HJ, Bhubalan K. Marine microplastics as vectors of major ocean pollutants and its hazards to the marine ecosystem and humans. Prog Earth Planet Sci. 2021;8:1–26.
8. Thompson RC, Olsen Y, Mitchell RP, Davis A, Rowland SJ, John AWG, et al. Lost at sea: where is all the plastic? Science. 2004;304(5672):838.
9. Cózar A, Echevarría F, González-Gordillo JI, Irigoien X, Úbeda B, Hernández-León S, et al. Plastic debris in the open ocean. Proc Natl Acad Sci. 2014;111(28):10239–44.
10. Eriksen M, Lebreton LCM, Carson HS, Thiel M, Moore CJ, Borerro JC, et al. Plastic pollution in the world's oceans: more than 5 trillion plastic pieces weighing over 250,000 tons afloat at sea. PLoS ONE. 2014;9(12):e111913.
11. Kaandorp MLA, Dijkstra HA, van Sebille E. Closing the Mediterranean marine floating plastic mass budget: inverse modeling of sources and sinks. Environ Sci Technol. 2020;54(19):11980–9.
12 Hammer J, Kraak MHS, Parsons JR. Plastics in the marine environment: the dark side of a modern gift. Rev Environ Contam Toxicol. 2012. https://doi.org/10.1007/978-1-4614-3414-6_1.
13. Galloway TS, Cole M, Lewis C. Interactions of microplastic debris throughout the marine ecosystem. Nat Ecol Evol. 2017;1(5):116.
14. Kaiser D, Kowalski N, Waniek JJ. Effects of biofouling on the sinking behavior of microplastics. Environ Res Lett. 2017;12(12):124003.
15. Harris PT. The fate of microplastic in marine sedimentary environments: a review and synthesis. Mar Pollut Bull. 2020;158:111398.
16. Hoseini M, Bond T. Predicting the global environmental distribution of plastic polymers. Environ Pollut. 2022;300:118966.
17 Giere O. The microscopic motile fauna of aquatic sediments. Heidelberg: Springer; 2009.
18 Heip C, Vincx M, Vranken G. The ecology of marine nematodes. Oceanogr Mar Biol Annu Rev. 1985; 23: 399-489.
19. Schratzberger M, Ingels J. Meiofauna matters: the roles of meiofauna in benthic ecosystems. J Exp Mar Biol Ecol. 2018;502:12–25.
20. Coull BC. Role of meiofauna in estuarine soft-bottom habitats. Aust J Ecol. 1999;24(4):327–43.
21. Moens T, Braeckman U, Derycke S, Fonseca G, Gallucci F, Gingold R, et al. Ecology of free-living marine nematodes. Berlin: Handbook of Zoology De Gruyter; 2013.
22. de França FJL, Moens T, da Silva RB, Pessoa GL, França DAA, Dos Santos GAP. Short-term microplastic effects on marine meiofauna abundance, diversity and community composition. PeerJ. 2024;12:e17641.
23. Fueser H, Mueller MT, Weiss L, Höss S, Traunspurger W. Ingestion of microplastics by nematodes depends on feeding strategy and buccal cavity size. Environ Pollut. 2019;255:113227.
24. Di Lorenzo T, Cabigliera SB, Martellini T, Laurati M, Chelazzi D, Galassi DMP, et al. Ingestion of microplastics and textile cellulose particles by some meiofaunal taxa of an urban stream. Chemosphere. 2023;310:136830.
25. Yu Y, Chen H, Hua X, Dang Y, Han Y, Yu Z, et al. Polystyrene microplastics (PS-MPs) toxicity induced oxidative stress and intestinal injury in nematode *Caenorhabditis elegans*. Sci Total Environ. 2020;726:138679.
26. Fueser H, Mueller MT, Traunspurger W. Ingestion of microplastics by meiobenthic communities in small-scale microcosm experiments. Sci Total Environ. 2020;746:141276.
27. Ma Y, You X. Microplastics in freshwater ecosystems: a significant force of disrupting health and altering trophic transfer patterns by reduced assimilation efficiency of aquatic organisms. Aquaculture. 2025;594:741463.
28. Redondo-Hasselerharm PE, Gort G, Peeters E, Koelmans AA. Nano-and microplastics affect the composition of freshwater benthic communities in the long term. Sci Adv. 2020;6(5):eaay4054.
29. Daché E, Zeppilli D, Sarrazin J, Singh R, Baldrighi E, Miljutin D, et al. MarNemaFunDiv: a first comprehensive dataset of functional traits for marine nematodes. Sci Data. 2025;12(1):752.
30. Coull BC. Pollution and meiofauna: field, laboratory, and mesocosm studies. Oceanogr Mar Biol Ann Rev. 1992;30:191–271.
31. Monteiro L, Moens T, Lynen F, Traunspurger W. Effects of the water-soluble fraction of a crude oil on freshwater meiofauna and nematode assemblages. Ecotoxicol Environ Saf. 2019;176:186–95.
32. Vafeiadou AM, Bretana BLP, Van Colen C, Dos Santos GAP, Moens T. Global warming-induced temperature effects to intertidal tropical and temperate meiobenthic communities. Mar Environ Res. 2018;142:163–77.
33. Wakkaf T, Allouche M, Harrath AH, Mansour L, Alwasel S, Ansari KGMT, et al. The individual and combined effects of cadmium, polyvinyl chloride (PVC) microplastics and their polyalkylamines modified forms on meiobenthic features in a microcosm. Environ Pollut. 2020;266:115263.
34. Austen MC, McEvoy AJ, Warwick RM. The specificity of meiobenthic community responses to different pollutants: results from microcosm experiments. Mar Pollut Bull. 1994;28(9):557–63.
35. Fueser H, Mueller MT, Traunspurger W. Rapid ingestion and egestion of spherical microplastics by bacteria-feeding nematodes. Chemosphere. 2020;261:128162.
36. Murrell MC, Fleeger JW. Meiofauna abundance on the Gulf of Mexico continental shelf affected by hypoxia. Cont Shelf Res. 1989;9(12):1049–62.
37. Moens T, Verbeeck L, Vincx M. Preservation and incubation time-induced bias in tracer-aided grazing studies on meiofauna. Mar Biol. 1999;133:69–77.
38. De Grisse A. Redescription or modifications of some techniques used in the study of plant parasitic nematodes. Meded Rijksuniv Landbouwwet Gent. 1969;34:351–69.
39. Warwick RM, Clarke KR. Taxonomic distinctness and environmental assessment. J Appl Ecol. 1998;35(4):532–43.
40. Platt HM, Warwick RM, Furstenberg JP. Free-living marine nematodes. part 1 British Enoplids. Taylor & Francis; 1985.

41. Platt HM, Warwick RM. Freeliving marine nematodes: Part II. British Chromadorida. Synopses of the British Fauna No. 38. 1988.
42. Wieser W. Die Beziehungen zwishen Mundhöhlengestalt, Ernährungsweise und Vorkommen bei freilebenden marinen Nematoden. Arkiv für Zoologie (Ser 2). 1953;4:439–84.
43. Bongers T. The maturity index: an ecological measure of environmental disturbance based on nematode species composition. Oecologia. 1990;83(1):14–9.
44. Bongers T, Ferris H. Nematode community structure as a bioindicator in environmental monitoring. Trends Ecol Evol. 1999;14(6):224–8.
45. Andrassy I. Die Rauminhalts- und Gewichtsbestimmung der Fadenwürmer (Nematoden). Acta Zool Hung. 1956;2(1):1–5.
46. Peng G, Xu P, Zhu B, Bai M, Li D. Microplastics in freshwater river sediments in Shanghai, China: a case study of risk assessment in mega-cities. Environ Pollut. 2018;234:448–56.
47. Klein S, Worch E, Knepper TP. Occurrence and spatial distribution of microplastics in river shore sediments of the Rhine-Main area in Germany. Environ Sci Technol. 2015;49(10):6070–6.
48. Shang X, Lu J, Feng C, Ying Y, He Y, Fang S, et al. Microplastic (1 and 5 μm) exposure disturbs lifespan and intestine function in the nematode *Caenorhabditis elegans*. Sci Total Environ. 2020;705:135837.
49. Lu Y, Yuan J, Lu X, Su C, Zhang Y, Wang C, et al. Major threats of pollution and climate change to global coastal ecosystems and enhanced management for sustainability. Environ Pollut. 2018;239:670–80.
50. Scherer C, Brennholt N, Reifferscheid G, Wagner M. Feeding type and development drive the ingestion of microplastics by freshwater invertebrates. Sci Rep. 2017;7(1):17006.
51. Huang G, Ma Y, Xie D, Zhao C, Zhu L, Xie G, et al. Evaluation of nanoplastics toxicity in the soil nematode *Caenorhabditis elegans* by iTRAQ-based quantitative proteomics. Sci Total Environ. 2023;862:160646.
52. Kang T, Kim D, Oh JH. Ingestion of microplastics by free-living marine nematodes, especially *Enoplolaimus* spp., in Mallipo Beach, South Korea. Plankton Benthos Res. 2021;16(2):109–17.
53. Buck JC, Weinstein SB, Young HS. Ecological and evolutionary consequences of parasite avoidance. Trends Ecol Evol. 2018;33(8):619–32.
54. Weihs D, Webb PW. Optimal avoidance and evasion tactics in predator-prey interactions. J Theor Biol. 1984;106(2):189–206.
55. Rauchschwalbe MT, Höss S, Haegerbaeumer A, Traunspurger W. Long-term exposure of a free-living freshwater micro- and meiobenthos community to microplastic mixtures in microcosms. Sci Total Environ. 2022;827:154207.
56. Calabrese EJ, Baldwin LA. Defining hormesis Hum Exp Toxicol 21: 91–97. Find this article online. 2002.
57. Mueller MT, Fueser H, Trac LN, Mayer P, Traunspurger W, Höss S. Surface-related toxicity of polystyrene beads to nematodes and the role of food availability. Environ Sci Technol. 2020;54(3):1790–8.
58. Bouleefah F, Nasri A, Hannachi A, Béjaoui M, Mahmoudi E. Insights into taxonomic and functional trait assessment of marine nematodes in mediterranean coastal ecosystems after exposure to polyethylene microplastics and sulfonamide antibiotics. Int J Environ Sci Technol. 2025;22(10):9005–20.
59. Corinaldesi C, Canensi S, Carugati L, Martire ML, Marcellini F, Nepote E, et al. Organic enrichment can increase the impact of microplastics on meiofaunal assemblages in tropical beach systems. Env Pollut. 2022;292:118415.
60. Warwick R. A new method for detecting pollution effects on marine macrobenthic communities. Mar Biol. 1986;92(4):557–62.
61. Moens T, Yeates GW, De Ley P. Use of carbon and energy sources by nematodes. Nematol Monogr Perspect. 2004;2:529-45.
62. Ridall A, Ingels J. Suitability of free-living marine nematodes as bioindicators: status and future considerations. Front Mar Sci. 2021;8:685327.
63. Losi V, Grassi E, Balsamo M, Rocchi M, Gaozza L, Semprucci F. Changes in taxonomic structure and functional traits of nematodes as tools in the assessment of port impact. Estuar Coast Shelf Sci. 2021;260:107524.
64. Sahraeian N, Riera R, Mantha G, Sahafi HH, Mosallanejad H. Divergent communities of marine nematodes in impacted beaches of Bandar Abbas (Iran). Mar Ecol. 2024;45(6):e12827.
65. Moens T, Vafeiadou AM, De Geyter E, Vanormelingen P, Sabbe K, De Troch M. Diatom feeding across trophic guilds in tidal flat nematodes, and the importance of diatom cell size. J Sea Res. 2014;92:125–33.
66 Salma J, Nasira K, Saima M, Shahina F. Morphological and molecular identification of four new species of marine nematodes. Pak J Nematol. 2017;35(2):113–50.
67. Huang Y, Xu K. A new species of free-living nematode of *Daptonema* (Monohysterida: Xyalidae) from the Yellow Sea, China. Aq Sci Tech. 2013;1(1):1–8.
68. Ahmed M, Holovachov O. Description of a new marine predatory nematode Latronema dyngi sp. nov.(Nematoda, Chromadorida, Selachinematidae) from the west coast of Sweden and an updated phylogeny of Chromadoria. Mar Biodivers. 2020;50(6):113.
69. Boufahja F, Beyrem H. Description of Marylynnia puncticaudata n. sp.(Nematoda, Cyatholaimidae) from Bizerte Lagoon, Tunisia. Anim Biodivers Conserv. 2014;37(2):205–16.
70. Costa E, Piazza V, Lavorano S, Faimali M, Garaventa F, Gambardella C. Trophic transfer of microplastics from copepods to jellyfish in the marine environment. Front Environ Sci. 2020;8:571732.

Publisher's Note